Archives of Microbiology (2022) 204:183
https://doi.org/10.1007/s00203-022-02784-2

ORIGINAL PAPER

Antibiotic-active heterotrophic *Firmicutes* sheltered in seaweeds: can they add new dimensions to future antimicrobial agents?

Kajal Chakraborty[1] · Chesvin Varghese[1,2] · Sumayya Asharaf[1] · Rekha Devi Chakraborty[3]

Received: 17 October 2021 / Revised: 22 January 2022 / Accepted: 28 January 2022 / Published online: 18 February 2022

Abstract

Appearance of drug-resistant microorganisms prompted researchers to unravel new environments for development of novel antimicrobial agents. Culture-supported analysis of heterotrophic bacteria associated with seaweeds yielded 152 strains, in that larger share of the isolates was embodied by *Bacillus atrophaeus* SHB2097 (54%), *B. velezensis* SHB2098 (24%), *B. subtilis* SHB2099 (12%), and *B. amyloliquefaciens* SHB20910 (10%). One of the most active strains characterized as *B. atrophaeus* SHB2097 (MW821482) with an inhibition zone more than 30 mm on spot-over-lawn experiment, was isolated from a seaweed *Sargassum wightii*, was selected for bioprospecting studies. Significant antibacterial potential was displayed by bacterial organic extract against vancomycin-resistant *Enterococcus faecalis*, *Pseudomonas aeruginosa*, methicillin-resistant *Staphylococcus aureus,* and *Klebsiella pneumonia* with minimum inhibitory concentration 6.25 µg/mL and comparable to the antibiotics ampicillin and chloramphenicol. The genes of type 1 *pks* (MZ222383, 700 bp) and hybrid *nrps/pks* (MZ222389, 1000–1400 bp) of *B. atrophaeus* MW821482 could be amplified. The bacterium displayed susceptibility to the commercially available antibiotic agents, and was negative for the pore-forming non-hemolytic hemolysin BL (*hbl*) and enterotoxin (*nhe*) genes, and therefore, was not pathogenic. The bacterium was found to possess genes (1000–1400 bp) involved in the biosynthesis of siderophore-class of compounds (MZ222387 and MZ222388) that showed 99% of similarity in BLAST search, and showed production of siderophore. Noteworthy antibacterial activities against clinically important pathogenic bacteria in conjunction with occurrence of genes coding for antimicrobial metabolites inferred that the marine heterotrophic bacterium *B. atrophaeus* SHB2097 could be used for the development of antibacterial agents against the emerging antibiotic resistance.

Keywords Seaweed-associated heterotrophic bacteria · *Bacillus atrophaeus* MW821482 · Antimicrobial · Drug-resistant pathogens · Polyketide synthetase

Introduction

Bacterial communities associated with seaweeds are valuable biotechnological resources as they yield a wide-ranging diversity of pharmaceutically active compounds (Zubia et al. 2009; Le Lann et al. 2016). The increase in antibiotic-resistant microorganisms and the necessity for new antimicrobials prompted researchers to look into novel habitations for bioactive substance production. The capacity of marine heterotrophic bacteria to provide biochemical protection to host eukaryotes in the face of predators and pathogenic organisms has been recognized (Kanagasabhapathy et al. 2006; Penesyan et al. 2009; Ali et al. 2012). While chemical defences have a propensity for displaying a significant part to establish the relationship between the marine eukaryotic host and their associated microorganisms, antimicrobial properties of marine organisms have

Communicated by Jorge Membrillo-Hernández.

Kajal Chakraborty and Chesvin Varghese are joint first author. They have equally contributed towards the outcome of this study.

✉ Kajal Chakraborty
kajal.chakraborty@icar.gov.in; kajal_cmfri@yahoo.com

[1] Marine Biotechnology Division, Central Marine Fisheries Research Institute, Ernakulam North, P.B. No. 1603, Cochin, Kerala State 682018, India

[2] School of Biotechnology, Amrita Vishwa Vidyapeetham, Vallikavu PO, Amritapuri, Kollam, Kerala State 690525, India

[3] Crustacean Fisheries Division, Central Marine Fisheries Research Institute, Ernakulam North, P.B. No. 1603, Cochin, Kerala State 682018, India

received little attention. Biotechnological and pharmacological sectors highlighted the ability of marine heterotrophic isolates as promising antimicrobial agents (Soria-Mercado et al. 2012; Kizhakkekalam and Chakraborty 2020).

Marine *Bacillus* were described to produce various bioactive metabolites (Fickers 2012), such as polyketides, nonribosomal peptides, macrolactones, among others (Cherian et al. 2019). A number of previous works envisaged to demonstrate antibiotic and antifouling activities of seaweed-related bacterial species (Penesyan et al. 2009; Wiese et al. 2009; Chakraborty et al. 2017). *Bacillus subtilis*, with 252 products so far, is among the leading producers of bioactive metabolites and products. The bioactives are mostly antibacterial in nature, such as bacitracin and rhizocticin, accounting for 61% of the amino acids and peptides (Chassagne et al. 2019). *Bacillus velezensis* was previously recognized as one of the biocontrol agents against phytopathogen (Kim et al. 2017; Chen et al. 2018; Francis and Chakraborty 2021; Chakraborty et al. 2021), even though it has recently developed into an antagonist against pathogens (Chen et al. 2018; Yi et al. 2018; Li et al. 2020). Nonribosomal peptide synthetases (NRPSs) and polyketide synthetases (PKSs), which are ubiquitous in *Proteobacteria*, *Firmicutes* and *Actinobacteria*, were found to catalyze the biosyntheses of bioactive natural products encompassing distinct structural architecture, and have been widely used for the development of biotechnological tools to evaluate bioactive bacteria (Kubanek et al. 2003; Wang et al. 2014). Previous reports of literature demonstrated the presence of biosynthetic genes, namely non-ribosomal peptide synthetase (*nrps*) and polyketide synthetase-I (*pks-I*) in heterotrophic bacteria (Chakraborty et al. 2014; Thilakan et al. 2016).

Herein, we have isolated the culturable heterotrophic bacteria related with seaweeds available at the Gulf-of-Mannar of peninsular India isolated by culture-reliant method, and assessed those for antimicrobial properties. Further, the selected bioactive isolate *Bacillus atrophaeus* SHB2097 (GenBank accession number MW821482) were characterized by morphological, biochemical and molecular techniques. Characteristic *nrps* and *pks-I* genes were analyzed by PCR amplification with degenerate primers, exploiting their conserved nature other than profiling its antimicrobial and hemolytic activities. Pathogenicity was assessed by in vitro hemolytic assay and presence of pore-forming non-hemolytic enterotoxin and hemolysin genes. *B. atrophaeus* SHB2097 was found to possess potential antimicrobial activities, and thus, its organic extract was assessed for antibacterial properties against selected pathogens coupled with its ability of siderophore production.

Materials and methods

Isolation of seaweed-associated heterotrophs

Seaweeds (class Phaeophyceae, Rhodophyceae, and Chlorophyceae) were accumulated by hand picking from the Gulf-of-Mannar region in Mandapam (9°17′0″ North, 79°7′0″ East), at low tide, and stored in seawater under sterile condition, as described earlier (Lemos et al. 1985). The brown seaweeds collected were *Sargassum wightii, Turbinaria conoides, Turbinaria ornata,* and *Turbinaria decurrens*, red seaweeds were *Gracilaria salicornia* and *Gracilaria edulis*, whereas *Ulva lactuca* was the green seaweed. Heterotrophic bacteria associated with the seaweeds were isolated by a formerly described method (Thilakan et al. 2016). Concisely, thallus parts of the seaweed samples (~ 1 g) were cleansed in sterile distilled water to eliminate the dirt and surface-associated microorganisms before being aseptically homogenized under suspended condition in sterile seawater (~ 100 mL) in a laminar airflow hood. Serial dilutions were made with the suspension, wherein sterile distilled water (9 mL) was added to the microbial suspension (1 mL), and various dilutions were prepared and plated on nutrient agar (NA) and Zobell Marine Agar (ZMA) supplemented with sodium chloride (NaCl, 1% w/v). The plates were incubated in the dark at 37 ± 1 °C for 1 week, and pure colonies were acquired by succeeding purification on NA added with common salt (1% w/v) (Chakraborty et al. 2014). While over 113 different colony phenotypes were observed, we have succeeded to isolate 75 strains as pure cultures. Colony morphology and pigments of these isolates in the incubated plates were recorded, and a total of 31 well-grown and morphologically distinct bacterial cultures were selected and sub-cultured into the sterile NA plates. The bacterial cultures were further quadrant-streaked to obtain the pure cultures, and single colonies were selected and streaked on NA slants. The isolates were incubated at 34 °C, and further stored at 20 °C in the BOD incubator (Labline, India). The pure cultures were inoculated into NA (with 1% NaCl) by stab method, and glycerol was added onto it. These glycerol stab stocks were stored in − 20 °C in the BOD incubator for long-term storage of the cultures (Ismail et al. 2018; Singh et al. 2011).

Preliminary antibacterial screening

The test pathogenic organisms used for preliminary screening of the heterotrophic bacteria were *Aeromonas salmonicida* (ATCC 27013), *Aeromonas caviae* (ATCC 15468), vancomycin-resistant *Enterococcus faecalis*

(ATCC 51299), *Aeromonas salmonicida* (ATCC 27013), *Aeromonas hydrophila* (ATCC 7966), methicillin-resistant *Staphylococcus aureus* (ATCC 33592), and *Vibrio parahaemolyticus* (ATCC 17802), which were procured from the American Type Culture Collection (Manassas, VA). *Vibrio parahaemolyticus* (MTCC 451), *Escherichia coli* (MTCC 443), *Yersinia enterocolitica* (MTCC 859), *Streptococcus pyogenes* (MTCC 1924), and *Edwardsiella tarda* (MTCC 2400) were obtained from the Microbial Type Culture Collection and Gene Bank (Institute of Microbial Technology, Chandigarh of India), whereas *Vibrio harveyi* (LMG 4044) type strain was procured from Sigma-Aldrich (St. Louis, MO). Upon receipt of the cultures, pathogenicity was judged by using PCR amplification with their explicit virulent features, whereas their characteristics were established by microbiological/biochemical and genotypic experiments, such as 16S rRNA sequence likeness (Armstrong et al. 2001). The pathogenic bacterial turf was grown on the plates of Mueller Hinton agar (MHA) (HiMedia, PA) and NA, over which the isolates were spotted using sterile swab. The plates were incubated at 37 °C, and the antibacterial activities were recorded by assessing the inhibition zone diameter using an antibiotic zone scale on the plates after 24, 48, and 72 h of incubation, by the spot-over-lawn antibacterial assay (Chakraborty et al. 2014; Kizhakkekalam and Chakraborty 2019).

Biochemical and molecular characterization of antibacterial isolates

The bacterial isolates with noteworthy antibacterial potential were characterized by microbiological and biochemical experiments (Krieg and Holt 1984). Morphological evaluation of the bacterial clusters was assessed on the agar plates, and standard checks, such as Gram staining, motility, reduction of nitrate/indole, Voges–Proskauer, citrate utilization, hydrolysis of gelatin/starch, etc. were performed. HiMedia Bacillus Identification kit including tests for malonate, ortho-nitrophenyl-β-galactoside, Voges–Proskauer, nitrate reduction, citrate, catalase, arginine, glucose, sucrose, trehalose, arabinose, and mannitol were used (supplementary material S1). The characteristics of the strains were substantiated by 16S rRNA gene system-centered phylogenetic examination supported by BLAST-likeness examination, and the biotyping was substantiated by matrix-assisted laser desorption/ionization-time of flight mass spectral analysis (MALDI/ToF by using a MALDI-TOF MS Biotyper, Microflex, Bruker Daltonics, Germany; version 3.1) and biolog characterization (GEN III Microplate and turbidimeter, Biolog) (Kanagasabhapathy et al. 2008) (supplementary material S1).

Genomic DNA of the bacteria was isolated using GenElute™bacterial genomic DNA isolation kit (Sigma-Aldrich, MO), whereas the quality of DNA was judged using a nanodrop biospectrophotometer (Eppendorf, Hamburg, Germany) by quantifying the absorbance at 260/280 nm, and the concentration of the sample (ng/μL) were observed. The 16S rRNA gene sequencing supported by BLAST resemblance search was used for molecular characterization. PCR reaction primer sequences were listed in Table 1. PCR was performed in the reaction mixture of PCR/(2X) master mix (12.5 μL), forward/reverse primer (1 μL both), DNA (1 ng), and the volume was adjusted to 0.025 mL using sterile water. PCR reactions were carried out in the thermo cycler (Biorad, CA) with the programming condition as follows: initial denaturation (94 °C for 5 min) subsequently 35 cycles (95 °C and 58 °C for 1 min each and 72 °C for 2 min), and an extension at 72 °C for 5 min. The 1 kb ladder on a 1.5% (w/v) agarose gel (in 1X TBE buffer) was used to assess molecular sizes of the amplified fragments (Thilakan et al. 2016), whereas the amplicons were sequenced for molecular identification before submitting in the GenBank. The sequenced data were analyzed against standard ones by BLAST program before being phylogenetically analyzed by MEGA X (Bioedit) (Kumar et al. 2018). Evolutionary history was resolved by neighbor-joining process centered on Kimura model and bootstrap study. Partial 16S rRNA gene sequences of the bacterial isolates were deposited in the GenBank (NCBI accession of MW821482, MW821799).

Molecular identification of functional genes

Identification of functional genes for *pks*-I, *nrps*, and siderophore in the most active strain was executed by PCR amplification of the specific genes using degenerate primers (Table 1). PCR was carried out in the reaction mixture comprehended in the earlier section as follows: denaturation at 94 °C for 5 min, subsequently 35 cycles at 95 °C for 1 min, annealing at 45 °C for 1 min for *pks*, and 55 °C for 1 min for *nrps*, subsequently extension at 72 °C for 5 min. PCR conditions for siderophore gene were fixed as primary denaturation 94 °C for 5 min, subsequently 30 cycles of 30 s/94 °C, 30 s/56 °C, 60 s/72 °C, and an extension at 72 °C for 5 min. The amplified PCR products were subjected to agarose gel electrophoretic (1.5%) analysis. The products (expected size of 700 bp for *pks-I* and 1000 bp for *nrps/siderophore*) were purified by an extraction kit (Gel Elute™, Sigma). The *pks-I* (MZ222383, 700 bp)/hybrid *nrps/pks* (MZ222389, 1000–1400 bp)*/siderophore* sequenced products (MZ222387 and MZ222388 1000–1400 bp) were deposited under the accession number MT394492 (in NCBI GenBank). The partial *pks-I*, *nrps* and *siderophore* sequences for *B. atrophaeus* SHB2097 were submitted to the NCBI GenBank. Amino acid sequence alignments with GenBank reference

Table 1 Polymerase chain reaction (PCR) primers used for 16S rRNA and *pks*, *nrps* gene and siderophore amplification

Primer[a]	Target gene[b]	Sequence (5′–3′)	Size of product (bp)	References
16S1	*16S rRNA*	GAGTTTGATCCTGGCTCA	1000	Xia et al. (2015)
16S2	*16S rRNA*	ACGGCTACCTTGTTACGACTT		
GCF	*Pks*	GCSATGGAYCCSCARCARCGSVT	700–1000	Schirmer et al. (2005)
GCR	*Pks*	GTSCCSGTSCRTGSSCYTCSAC		
GBF	*Pks*	RTRGAYCCNCAGCAICG	700–1000	Zhang et al. (2009)
GBR	*Pks*	VGTNCCNGTGCCRTG		
KS11F	*Pks*	GCIATGGAYCCICARCARMGIVT	700–1000	Schirmer et al. (2005)
KS12R	*Pks*	GTICCIGTICCRTGISCYTCIAC		
KSDPQQF	*Pks*	MGNGARGARGCNNWNSMNATGGAYCCNCARCANMG	700–1000	Zhang et al. (2009)
KSHSGDR	*Pks*	GGRTCNCCNARNSWNGTNCCNGTNCCRTG		
MTF	*Nrps*	GCNGGYGGYGCNTAYGTNCC	700–1000	Zhao et al. (2011)
MTR	*Nrps*	CCNCGDATYTTNACYTG		
SF	*Siderophore*	GACTGGATCCCACTAAACTGACCCTAGAGATGACCTCG	1000–1400	Christine et al. (2010)
SR	*Siderophore*	AAAGTGACTGGGTAACAGGGCGATTATCTGCACAACGTCTGC TCCATTG		
PF	*Siderophore*	GACTGGATCCCACTAAACTGACCCTAGAGATGACCTCG	1000–1400	Datta and Chakrabartty (2014)
PR	*Siderophore*	AAAGTGACTGGGTAACAGGGCGATTATCTGCACAACGTCTGC TCCATTG		

[a]The primer sequences used for the PCR reaction have been represented. PCR was performed in a total volume of 25 µL containing 1X reaction buffer with $MgCl_2$ (Sigma), 0.25 mM of each dNTP (Sigma), 0.5 mM of each primers (Sigma), 1 ng DNA and 0.3 U Taq DNA polymerase (Sigma)

[b]Phylogenetic analysis was carried out using 16S rRNA sequencing. Different sets of degenerate primers targeting genes encoding *pks-I* and *nrps* were used as described in the text. All of the amplification products were examined by agarose gel electrophoresis, and bands of 700–800 bp and 1000–1400 bp were classified as products of *pks-I* and *nrps* genes, respectively

sequences were performed for phylogenetic study (Zhu et al. 2009) and evolutionary history was deduced (Whelan and Goldman 2001; Tamura et al. 2011; Jones et al. 1992).

Antibiotic susceptibility, siderophore production, and toxicity assessment

Antibiotic sensitivity of *B. atrophaeus* SHB2097 was found out using commercially available antibiotic-permeated octadiscs (HiMedia Laboratories LLC, PA) (Kizhakkekalam et al. 2020, CLSI, 2009). Chrome azurol sulfonate (CAS) analysis was used to deduce the presence of siderophore (Louden et al. 2011) (supplementary material S2). Siderophore biosynthetic genes were characterized in the bacterial genome of *B. atrophaeus* SHB2097, and the sequences were deposited in the NCBI GenBank (MZ222387 and MZ222388). Toxicity of *B. atrophaeus* SHB2097 was assessed in vitro hemolytic assay (Gao et al. 2000) by streaking pure culture of the isolated bacterium on sheep blood agar plates (Kizhakkekalam and Chakraborty 2019), and by inspecting the presence of enterotoxin genes in the candidate bacterium (supplementary material S2) with reference to a *Streptococcus pyogenes* MTCC1924 as a control. Presence of pore-forming non-hemolytic enterotoxin (*nhe* A–C), and hemolysin BL (*hbl* A–D) genes was ascertained using PCR. The primers used to amplify the enterotoxin genes are shown in Table 2.

Sporulation efficiency

The culture of *B. atrophaeus* SHB2097 was prompted to sporulate by the nutrient depletion technique (Nicholson and Setlow 1990), wherein bacterial suspension (300 µL) was filled into a multi-well plate, and the absorbance was evaluated at 600 nm for every half an hour for a period of 48 h using a microplate reader (Multiskan-GO model 1510, Thermo Scientific, MA). The time was noted at which the bacterial culture reached their death phase in the exhaustion medium, as the commencement of sporulation. Following 48 h of incubation, the cultures were acquired by centrifugation (9500×*g*, 15 min), and the lysozyme treatment followed by salt and detergent washes were used for the purification of spores. Further, sterile

Table 2 Polymerase chain reaction (PCR) primers used for hemolysis gene amplification

Genes	Primer	Sequence (5′–3′)	Reference
hblA	HAF	ATGATAAAAAAAATCCCTTACAA	Sastalla et al. (2013)
	HAR	TTTGTGGAGTAACAGTTTCTACTT	
hblB	HBF	AAGCAATGGAATACAATGGG	Sastalla et al. (2013)
	HBR	AATATGTCCCAGTACACCCG	
hblC	HCF	GATACCAATGTGGCAACTGC	Sastalla et al. (2013)
	HCR	TTGAGACTGCTCGCTAGTTG	
hblD	HDF	ACCGGTAACACTATTCATGC	Sastalla et al. (2013)
	HDR	GAGTCCATATGCTTAGATGC	
nheA	NAF	GCTCTATGAACTAGCAGGAAAC	Hwang and Park (2015)
	NAR	GCTACTTACTTGATCTTCAACG	
nheB	NBF	TTTAGTAGTGGATCTGTACGC	Hwang and Park (2015)
	NBR	TTAATGTTCGTTAATCCTGC	
nheC	NCF	TGGATTCCAAGATGTAACG	Hwang and Park (2015)
	NCR	ATTACGACTTCTGCTTGTGC	

PCR was performed with the following run: a starting cycle of 2 min at 94 °C, followed by 35 cycles of 1 min at 94 °C, 1 min at 58 °C, and 2 min at 72 °C, and a final extension of 5 min at 72 °C

deionized water was used to suspend the bacterial spores before being proceeded with the final purification step, wherein the spore suspension was subjected to heating at 80 °C for 10 min, to confirm the removal of vegetative cells. The spore suspension was diluted by tenfold with maximum recovery diluent (Merck, Darmstadt, Germany), and plated on the brain heart infusion agar by spread plating method before incubating at 37 °C for two days so as to determine the total viable counts. Sporulation efficacy of the studied heterotrophic *Bacillus* was evaluated as percentage survival after heating.

Development of bacterial crude extracts and bioactivity assessment

B. atrophaeus SHB2097 possessing potential antimicrobial properties against pathogens, was extracted with ethyl acetate to produce extracellular bacterial extract. Briefly, *B. atrophaeus* was cultured over NA with 1–2% NaCl (at pH 8, 30 °C for 3 days), and the incubation period was ascertained from the bacterial growth kinetics to produce secondary metabolites. The symbiotic bacteria discharge the bioactive compounds in the agar growth medium, the agar containing extracellular metabolites was extracted with solvent ethyl acetate (~ 2500 mL) under reflux at a temperature below 80 °C on a water bath. The extract (~ 5.4 L) was subjected to dehydration by using anhydrous sodium sulfate (0.5 kg) before being concentrated by a rotary vacuum evaporator (Heidolph, Schwabach, Germany) at 40 °C (Kizhakkekalam and Chakraborty 2019). The bacterial organic extract (~ 5 g) was analyzed for in vitro bioactive potential. Antibacterial properties of the organic extract against clinically acknowledged pathogens were assessed by disc diffusion on Mueller Hinton agar plates and minimum inhibitory concentration (MIC) by microdilution method (Kizhakkekalam and Chakraborty 2019; Bauer et al 1966; Chakraborty et al. 2021). Iron chelation properties of the solvent extract of *B. atrophaeus* SHB2097 were assessed using ferrous ion (Fe^{2+}) chelating method (Gülçin 2007). The concentration of bacterial extract required to realize 50% Fe^{2+} chelating capacity was deliberated as IC_{50} (effective concentration) (supplementary material S3).

Data analysis and accession numbers

Statistical Program for Social Sciences (SPSS Inc, CA; ver. 10.0) was used for analyzing the data. Experiments were carried out in triplicate, and means of the parameters were computed for significance ($p \leq 0.05$) by analysis of variance. Partial 16S rRNA gene sequences were deposited in the GenBank (accession numbers of MW821482–821799). Partial *pks* sequences for *B. atrophaeus* MW821482 were deposited under the accession numbers MZ222383, MZ222384, MZ222385, MZ222386, whereas *nrps* gene sequence was deposited in the GenBank as MZ222389. Coding sequences for siderophore biosynthetic genes were deposited under the accession numbers MZ222387 and MZ222388.

Results

Isolation of seaweed-associated bacteria and antimicrobial assessment

Seven different intertidal macroalgae (otherwise termed as seaweeds) representing *Sargassum wightii, Turbinaria conoides, Gracilaria salicornia, Ulva lactuca, Turbinaria ornata, Turbinaria decurrans,* and *Gracilaria edulis*

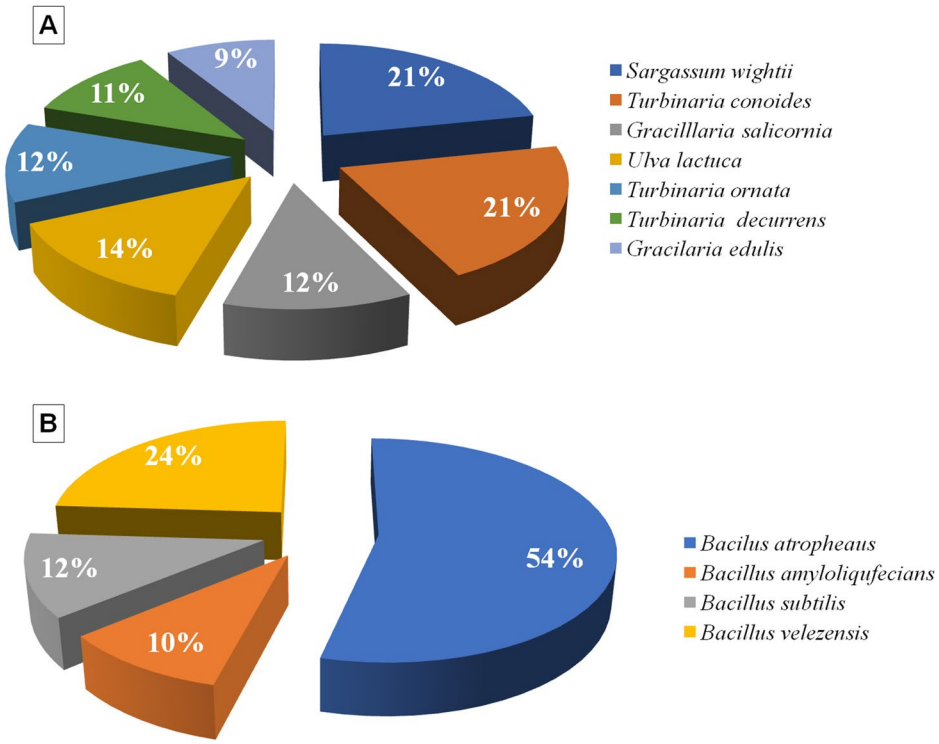

Fig. 1 Pie diagrams displaying the **A** dispersal of seaweed-associated heterotrophic bacteria contributed by the characteristic hosts and **B** contribution (percent segment to aggregate bacterial isolates with potential antibacterial properties against pathogens) of the bacteria in seaweed association

belonging to the families of Phaeophyceae, Chlorophyceae, and Rhodophyceae were harvested from the intertidal zones (Fig. 1A). One hundred and fifty-two heterotrophic bacterial isolates were purified to homogeneity by culture-dependent studies, whereas a total of 21% of those was isolated from *S. wightii* and *T. conoides* (Fig. 1B). The heterotrophic bacteria belonged to *B. atrophaeus* SHB2097 (54%), *B. velezensis* SHB2098 (24%), *B. subtilis* SHB2099 (12%), and *B. amyloliquefaciens* SHB20910 (10%) that were assessed for antibacterial properties against a wide range of drug-resistant pathogens. From the isolates, three strains of *B. atrophaeus* and one each of *B. velezensis* isolated from *S. wightii* and *T. conoides* were purified to homogeneity, showed potential antibacterial properties {inhibition zone diameter of 32–40 mm, against MRSA (Fig. 2A) and *V. parahaemolyticus* (Fig. 2B)}. Among various macroalgal species considered in the present study, two bioactive isolates *B. atrophaeus* (MW821482) and *B. velezensis* (MW821799), which were capable of enduring sub-culturing for laboratory culture conditions, showed general antagonistic activities against the studied pathogens (Fig. 2B). Pure bacterial colonies, which were susceptible to antibiotics (Fig. S1), were preserved at −80 °C under sterile glycerol stab.

Characterization of potential bioactive strains and 16S rRNA-based phylogeny

Morphological, microbiological and biochemical attributes of the studied bacteria are listed in Table S1–S2, which enabled the classification under the genus of *Bacillus*, whereas 16S rRNA gene sequencing led to the characterization at species level as *B. atrophaeus* SHB2097 and *B. velezensis* SHB2098 (Fig. 2C). The bacteria were classified as Gram positive by potassium hydroxide/Gram staining experiments. White lobed margins with casein hydrolyzing and nitrate reduction properties characterized *B. atrophaeus* SHB2097 (Table S1–S2). *B. velezensis* SHB2098 was found to develop a dark brown pigmentation at the later stage of exponential growth phase (Turick et al. 2008). *B. velezensis* SHB2098 grown at its optimum with 1–4% NaCl at a temperature and pH of about of 30 °C and 8.0, respectively, whereas *B. atrophaeus* SHB2097 was found to grow at its optimum at the pH range of 7–9, when incubated at 37 °C. Features of biochemical reactions for biolog characteristics of *B. atrophaeus* SHB2097 and *B. velezensis* SHB2098 were also detailed (Table S3-S4). MALDI–TOF biotyping certainty score of 2.152 and 1.953 for high abundance ribosomal proteins (Seng et al. 2009) of *B. velezensis* SHB2098 and *B. atrophaeus* SHB2097, respectively, further corroborated the characterization (Fig. S2-S3). The above strains were subjected to 16S rRNA genotyping (GenBank accession numbers of MW821482 for *B. atrophaeus* SHB2097 and MW821799 for *B. velezensis* SHB2098) (Fig. S4), and the sequences were harmonized with the contiguous lineages recorded in the GenBank to build a phylogenetic tree. Evolutionary lineage was construed by maximum likelihood mode (Tamura et al. 2011), and the tree with maximum logarithm of probability was presented.

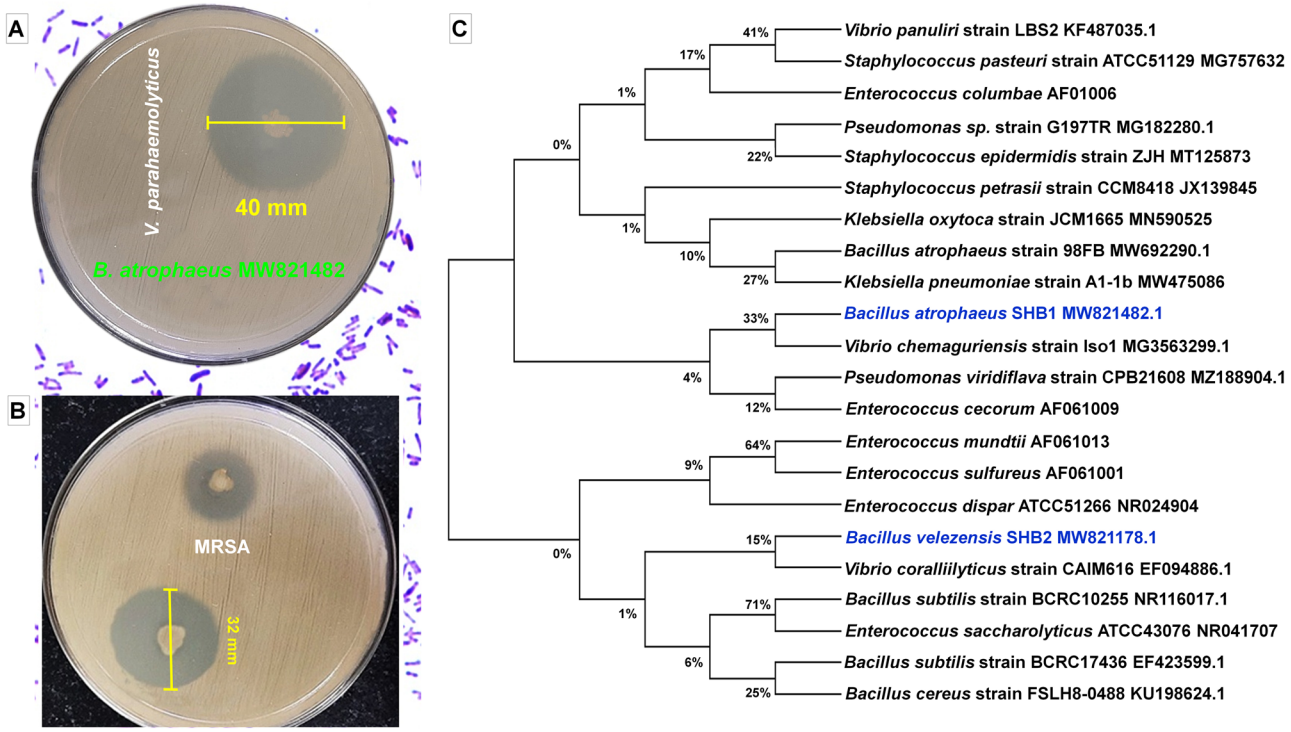

Fig. 2 **A** Antibacterial activity displayed by *B. atrophaeus* SHB2097 (GenBank accession number MW821482) and **B** *B. velezensis* SHB2098 (GenBank number: MW821799) against *V. parahaemolyticus* and MRSA (diameter of zone of growth inhibition, 40 mm and 32 mm, respectively) as visualized on MHA plates by spot-on-lawn assay. **C** Phylogenetic tree from partial 16S rRNA sequences between the studied isolates and related species. The isolates were categorized as *B. atrophaeus* (SHB2097) and *B. velezensis* (SHB2098)

Analyses of *pks*, *nrps* and phylogenetic structure

Type-1 *pks* and *nrps* genes were amplified in *B. atrophaeus* SHB2097 and *B. velezensis* SHB2098 (Fig. S5), and the sequence showing substantial BLAST-likeness was deposited in the GenBank (accession number MZ222383) (Fig. 3). The PKS-specific primers could successfully obtain the PCR amplicons (~ 700 bp) displaying substantial analogy to the sequences submitted in the GenBank. The positive amplicons exhibited 99% likeness in sequence with those in hybrid *nrps/pks* gene of *B. velezensis* SHB2098 and type 1 *pks* gene of *B. atrophaeus* SHB2097, as observed in the blast analysis. Phylogeny of the KS domains in *B. atrophaeus* SHB2097 categorized the inferred sequences of amino acid as bacterial PKSs type I and for *B. velezensis* SHB2098 as NRPS/PKS hybrid (Fig. 3).

Siderophore production and ferrous ion chelation by *B. atrophaeus* SHB2097

A yellow hallow of about 32 mm diameter on CAS agar experiment recognized the production of siderophore by *B. atrophaeus* SHB2097 (Fig. 4B). Presence of siderophore biosynthetic genes was predicted, wherein one of the genes (1626 bp, GenBank accession number of MZ222387) could decode to (2,3-dihydroxybenzoyl) adenylate synthetase, while other gene (786 bp, MZ222388) was turned into dihydro-dihydroxybenzoate-NAD^+ oxidoreductase. Evolutionary pedigree was deduced, and the tree with maximum logarithm of probability was illustrated (Fig. 4D). Extracellular extract of *B. atrophaeus* SHB2097 showed potential ferrous ion chelation capacity (IC_{50} 4.2 mg/mL).

Toxicity assessment and sporulation efficiency

Presence of enterotoxin genes *nhe* (A–C) and *hbl* (A–D) were ascertained using PCR. Amplification for *nhe* (A–C) and *hbl* (A–D) were not observed proving that the bacterium *B. atrophaeus* SHB2097 did not have the hemolysis capacity. The pathogenic strains were amplified due to the presence of *nhe* and *hbl* genes, and therefore, displayed hemolysis activity. List of genes used for the amplification is summarized in Table 2. It was recognized that *B. atrophaeus* SHB2097 possessed spore-forming ability (Fig. 5E).

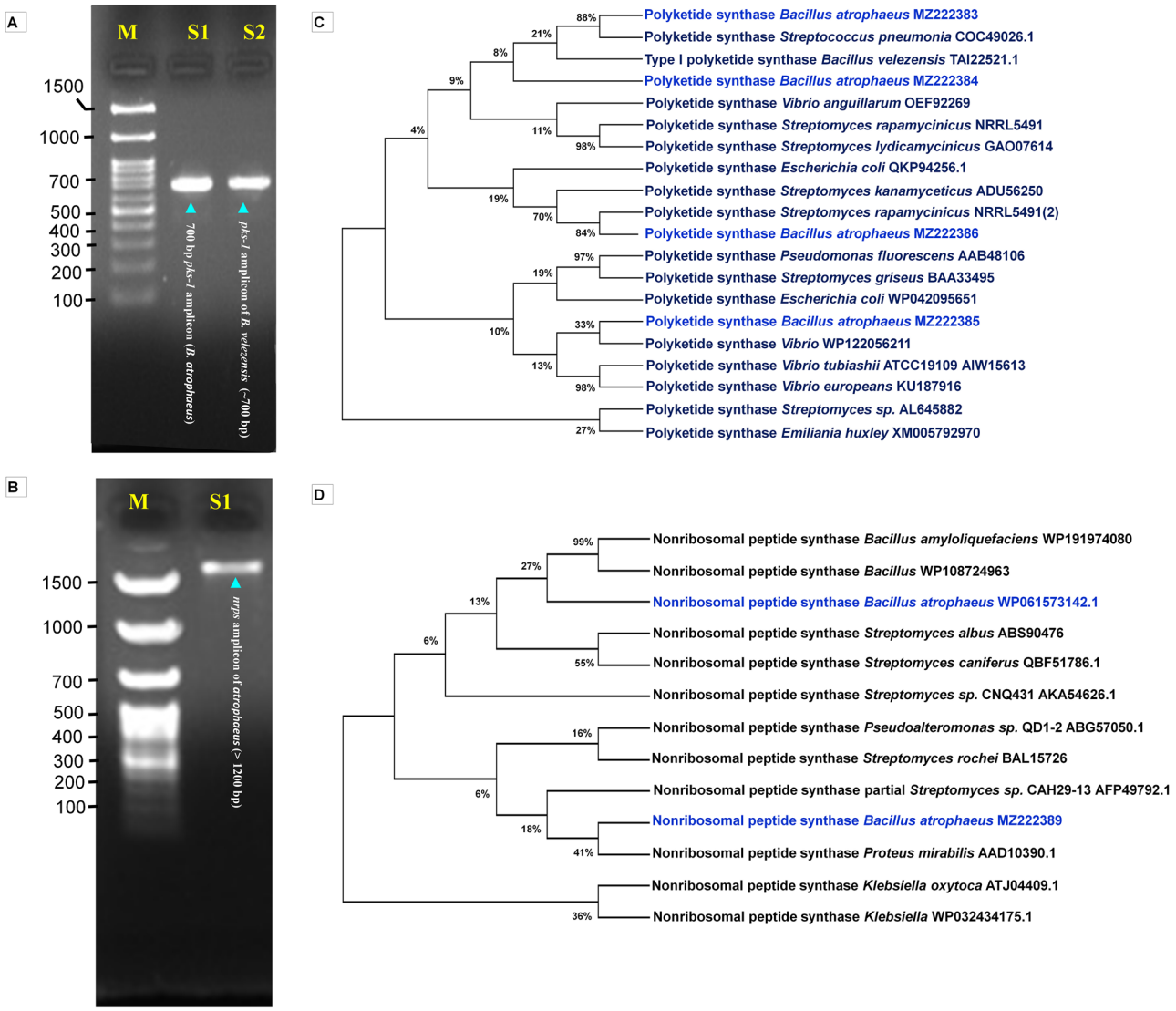

Fig. 3 **A** Polyketide synthase and **B** non-ribosomal peptide synthetase gene (*nrps*) products (~700 bp) of the antimicrobial bacterium *B. atrophaeus* SHB2097 associated with *S. wightii*. (S1) type I polyketide synthase gene (*pks*-I) product (~700 bp) of *B. velezensis* SHB2098 associated with *T. conoides* (T1). The amplified gene sequences for type I *pks* and *nrps* were submitted in the GeneBank with accession numbers of MZ222383, MZ222384, MZ222385 and MZ222386 for *pks* and MZ222389 for *nrps*, respectively. **C**, **D** Molecular phylogeny of ketosynthase domains as *pks* types I–III, *nrps* and hybrid of genes

Antibacterial potential of *B. atrophaeus* SHB2097 organic extract

Growth kinetics of *B. atrophaeus* SHB2097 for expression of bioactivity showed that antibacterial activity peaked (38 mm zone of inhibition against MRSA) following 56 h of incubation (Table 3, Fig. 5). Consequently, extracellular metabolites were recovered by incubating the cells for 60 h before being extracted with ethyl acetate to acquire the organic extract of *B. atrophaeus* (~5 g). Antimicrobial potential of the organic extract displayed 38 and 28 mm of inhibition zone against MRSA ATCC 33952 and *S. pyogens* MTCC 1924, respectively, and 32 mm against *V. parahaemolyticus* (Fig. 5A–C) in comparison to chloramphenicol (15 mm inhibition zone against *V. parahaemolyticus*). It was apparent that the MIC of *B. atrophaeus* SHB2097 organic extract was 6.25 µg/mL

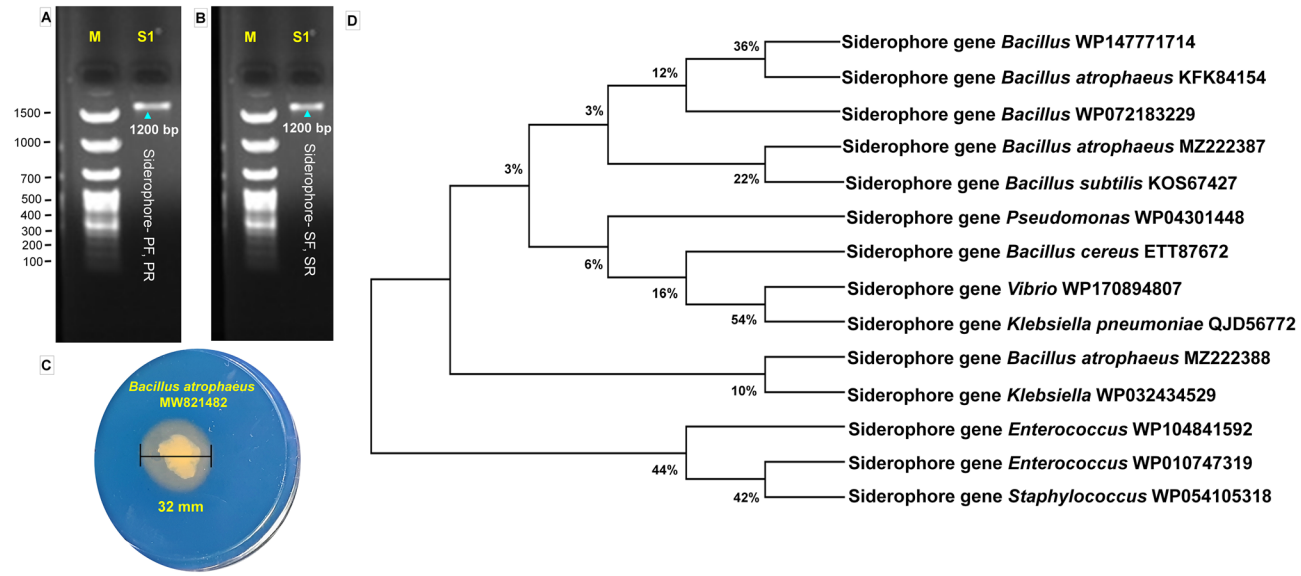

Fig. 4 **A–B** Siderophore genes *PF, PR* and *SF*, *SR* amplified for *B. atrophaeus* SHB2097 (S1) were shown. **C** Indicative photograph showing the production of siderophore by *B. atrophaeus* SHB2097 on CAS agar plate with zone of clearance of 32 mm. **D** Molecular phylogeny analysis of the siderophore genes *PF*, *PR* and *SF*, *SR* by *B. atrophaeus* SHB2097 were submitted in the GenBank with the respective accession numbers as MZ222387, MZ222388

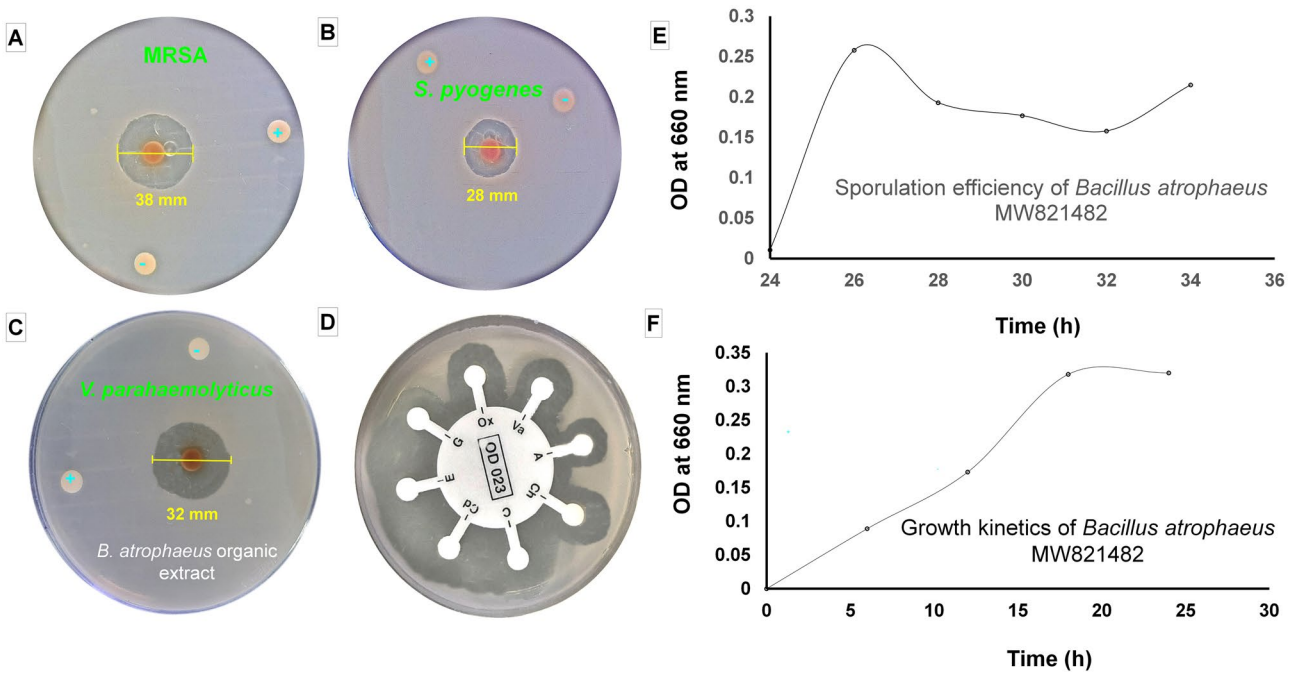

Fig. 5 Antimicrobial properties of the bacterial extracts of *B. atrophaeus* SHB2097 against **A** methicillin-resistant *S. aureus*, **B** *S. pyogenes,* and **C** *V. parahaemolyticus.* **D** Indicative photograph representing the antibiotic susceptibility test (with octadisc) result of bacteria *B. atrophaeus.* The octadisc comprised of eight antibiotics, ofloxacin, penicillin-G, clindamycin, cephalothin, trimoxazole, vancomycin, gentamicin, and erythromycin positioned on the center of the MHA plate with the culture of candidate bacteria (after the guidelines of Clinical and Laboratory Standard Institute guidelines, CLSI, 2009). **E**, **F** Graphs representing bacterial growth kinetics and sporulation efficiency of the selected isolate *B. atrophaeus* SHB2097 at 660 nm

Table 3 Antibacterial activities of seaweed-associated heterotrophic bacteria against pathogens

Test pathogens	Antimicrobial activity against test pathogens; inhibition zone (mm)			
	Sargassum wightii		*Turbinaria conoides*	
	B. atrophaeus MW821482 (S1)	*B. atrophaeus* MW821483 (S2)	*B. atrophaeus* MW821798 (T1)	*B. velezensis* MW821799 (T2)
Vibrio parahaemolyticus (MTCC 451)	$40^{a} \pm 0.25$	$38^{c} \pm 0.30$	$40^{b} \pm 0.21$	$37^{d} \pm 0.44$
Methicillin-resistant *Staphylococcus aureus* (ATCC 33592)	$32^{a} \pm 0.35$	$22^{c} \pm 0.10$	$18^{d} \pm 0.28$	$24^{b} \pm 0.50$
Vancomycin-resistant *Staphylococcus aureus*	$36^{a} \pm 0.22$	$26^{d} \pm 0.41$	$30^{c} \pm 0.20$	$33^{b} \pm 0.25$
Escherichia coli (MTCC 443)	$18^{c} \pm 0.20$	$22^{b} \pm 0.60$	$16^{d} \pm 0.11$	$28^{a} \pm 0.44$
Aeromonas salmonicida (ATCC 27013)	$39^{a} \pm 0.40$	$34^{b} \pm 0.32$	$26^{d} \pm 0.14$	$32^{c} \pm 0.47$
Edwardsiella tarda (MTCC 2400)	$26^{b} \pm 0.28$	$17^{d} \pm 0.12$	$28^{a} \pm 0.30$	$22^{c} \pm 0.24$
Streptococcus pyogenes (MTCC 1924)	$20^{c} \pm 0.26$	$21^{b} \pm 0.13$	$27^{a} \pm 0.15$	$18^{d} \pm 0.81$
Aeromonas caviae (MTCC 646)	$16^{c} \pm 0.81$	$15^{d} \pm 0.20$	$23^{a} \pm 0.12$	$21^{b} \pm 0.82$
Vancomycin-resistant *Enterococcus faecalis* (ATCC 51299)	$26^{a} \pm 0.30$	$19^{d} \pm 0.47$	$23^{b} \pm 0.81$	$21^{c} \pm 0.81$
Vibrio harveyi (LMG 4044)	$21^{c} \pm 0.81$	$18^{d} \pm 0.62$	$22^{b} \pm 0.55$	$24^{a} \pm 0.40$
Yersinia enterocolitica (MTCC 859)	$22^{b} \pm 0.20$	$23^{a} \pm 0.81$	$16^{c} \pm 0.30$	$12^{d} \pm 0.70$
Aeromonas hydrophila (ATCC 7966)	$28^{a} \pm 0.18$	$21^{b} \pm 0.50$	$18^{d} \pm 0.70$	$20^{c} \pm 0.63$

Data were expressed as mean ± standard deviation of three replicates

Means followed by different superscripts (a–d) within the same row indicate significant difference ($p < 0.05$)

Table 4 Antibacterial activities of the organic extract of *B. atrophaeus* SHB2097 against pathogenic bacteria

Test pathogens	*B. atrophaeus* organic extract		Chloramphenicol	
	Inhibition zone (mm)[k]	MIC (MBC)[l]	Inhibition zone (mm)[k]	MIC (MBC)[l]
Vibrio parahaemolyticus (MTCC 451)	$32^{a} \pm 0.42$	6.25 (6.25)	$15^{a} \pm 0.20$	6.25 (6.25)
Methicillin-resistant *Staphylococcus aureus* (ATCC 33592)	$38^{b} \pm 0.16$	6.25 (6.25)	$11^{b} \pm 0.11$	6.25 (6.25)
Vancomycin-resistant *Staphylococcus aureus*	$22^{d} \pm 0.49$	6.25 (12.5)	ND	12.5 (12.5)
Escherichia coli (MTCC 443)	$19^{e} \pm 0.23$	6.25 (6.25)	$8^{c} \pm 0.23$	12.5 (12.5)
Auromonas salmonicida (ATCC 27013)	$24^{c} \pm 0.47$	6.25 (6.25)	$9^{c} \pm 0.32$	6.25 (6.25)
Edwardsiella tarda (MTCC 2400)	$18^{f} \pm 0.20$	12.5 (12.5)	$10^{b} \pm 0.20$	12.5 (12.5)
Streptococcus pyogenes (MTCC 1924)	$28^{b} \pm 0.30$	12.5 (12.5)	ND	6.25 (6.25)
Aeromonas caviae (MTCC 646)	$12^{j} \pm 0.58$	6.25 (6.25)	$10^{b} \pm 0.23$	12.5 (12.5)
Vancomycin-resistant *Enterococcus faecalis* (ATCC 51299)	$14^{i} \pm 0.46$	12.5 (12.5)	ND	12.5 (12.5)
Vibrio harveyi (LMG 4044)	$17^{g} \pm 0.31$	12.5 (12.5)	$8^{c} \pm 0.23$	6.25 (6.25)
Yersinia enterocolitica (MTCC 859)	$14^{i} \pm 0.24$	6.25 (6.25)	$9^{c} \pm 0.32$	6.25 (6.25)
Aeromonas hydrophila (ATCC 7966)	$16^{h} \pm 0.17$	6.25 (6.25)	$10^{b} \pm 0.20$	12.5 (12.5)

Data were expressed as mean ± standard deviation of three replicates

ND non-detectable zone of clearance

[a–j]Column-wise values with different superscripts of this type indicate significant difference ($p < 0.05$). Triplicate values were taken and the variance analyses (ANOVA) were carried out (using Statistical Program for Social Sciences 13.0) for means of all parameters to examine the significance level ($p < 0.05$)

[k]30 µg/mL of crude extract

[l]MBC values of *B. atropheus* and chloramphenicol were described in parentheses, and expressed as µg/mL

against majorities of these pathogens (Table 4). MBC was noted with 6.25 µg/mL for *B. atrophaeus* SHB2097 against MRSA.

Discussion

Occurrence of microbial resistance to the prevalent antimicrobial agents and antibiotics led to the search for novel antimicrobial agents. Constant pursuit for newer

pharmacophore leads could pave the system to discover high-value compounds and drugs from microbes (Pandey 2019). Seaweeds or marine macroalgae were found to have chemical defense mechanisms against pathogens, and the substantial share of seaweed-associated bioactive heterotrophs shape a treasured source of pharmaceutical leads (Zheng et al. 2005; Vijayalakshmi et al. 2008). Lately, marine macroalgae-associated heterotrophs have attracted the marine microbiologists and biochemists in view of their potentials to biosynthesize bioactive compounds of various classes with pharmacological implications (Winter et al. 2013).

Bacteria associated with seaweeds were obtained from the Gulf-of-Mannar, as the intertidal heterotrophs were described to biosynthesize distinctive specialized metabolites in reaction to the stress conditions. Comprehensive findings of surface-associated bacteria isolated from the seaweeds were firstly described before the nineteenth century (Penesyan et al. 2009). It was found that the percentage of bioactive bacteria with potential antibacterial properties, associated with seaweeds and other marine organisms was more (11%) compared to those living in sediments and seawater (Zheng et al. 2005; Gram et al. 2010). Between the total of 152 bacterial isolated strains in the present study, *Gammaproteobacteria* and *Firmicutes* presented the largest communities. The phylum *Proteobacteria* was found to be the present in large quantities as hetrotrophic association with seaweeds, followed by *Actinobacteria, Bacteroidetes*, *Firmicutes* and *Chlorofexi* (Armstrong et al. 2001; Longford et al. 2007). Among the different seaweed species considered in this study, *Sargassum wightii* and *Turbinaria conoides* contributed bacterial isolates with potential bioactivities against the test pathogens. The share of bioactive isolates from seaweed hosts has been depicted in Fig. 2. Remarkably, the genera belonging to *Firmicutes* were plentiful, and majority of which were *B. atrophaeus* SHB2097 followed by *B. velezensis* SHB2098 (54 and 24% of the active isolates, respectively). *Bacillus subtilis* SHB2099 and *B. amyloliquefaciens* SHB20910 contributed the shares of 12 and 10% of the collective number of bioactive isolates associated with the seaweeds (Fig. 1).

Previous literature reports described the potential antimicrobial properties of seaweed-associated heterotrophic bacteria against drug-resistant pathogens, such as methicillin-resistant *Staphylococcus aureus* (MRSA) and vancomycin-resistant *Enterococcus faecalis* (VREfs) (Thilakan et al. 2016; Kizhakkekalam et al. 2020). With the aim of assessing the bioactive capability of the seaweed-associated isolates, they were evaluated for antibacterial properties by spot-over-lawn assay, wherein 57% of isolates were selected initially, and those isolates showed positive result towards the preliminary screening. The bacteria isolated from brown seaweeds, *S. wightii* and *T. conoides* showed greater activities among all the isolates. The bacterial isolates displaying broad-continuum of antimicrobial activities against nosocomial pathogens were selected for advanced studies (Fig. 2; Table 1). *B. atrophaeus* SHB2097 and *B. velezensis* SHB2098 (family *Firmicutes*), isolated from the brown seaweeds *S. wightii* and *T. conoides*, respectively, showed significant antagonistic potential against MRSA, VREfs, *A. salmonicida* and *V. parahaemolyticus* with zones of inhibition of 26–40 mm. Conspicuously, *Bacillus* sp. were ubiquitous on the surface of marine macroalgae, and were known to produce bioactive metabolites of biotechnological and pharmaceutical importance (Goecke et al. 2010).

Marine-derived *Bacillus* sp. were known to biosynthesize potential antimicrobial substances, for example cyclic peptides, polyketides, bacteriocins, and polyketide–peptide hybrids (Goecke et al. 2010) by non-ribosomal peptide synthetase (*nrps*), polyketide synthase (*pks*), and *nrps-pks* hybrid (Brakhage 2012; Wang et al. 2014). The β-lactam antibiotics, lipopeptide antibiotic daptomycin, and cyclosporine were produced by *nrps* (Felnagle et al. 2008; Doekel et al. 2008). Herein, the *pks* gene amplified for *B. atrophaeus* SHB2097 (GenBank ID MZ222383, MZ222384, MZ222385, MZ222386) revealed likeness to type I *pks* (Fig. 3). These cluster of genes were accountable to produce bacterial polyketide and lipopeptide metabolites (Aleti et al. 2015). Recently elucidated whole genome mining study showed that more than 30% of the *Bacillus* species were assessed to accommodate in the *pks*/*nrps* gene metabolite groups, while *nrps* and hybrid *nrps/pks* or *pks* shared a proportion of 7:3 of these encoded genes (Wang et al. 2014). Previous reports in bacteria associated with sponges also deduced the presence of *pks* gene (Zhu et al. 2009; Zhang et al. 2009). Presently, KS domain sequence-built phylogeny bundled four sequences with *B. atrophaeus* SHB2097. Hence, the sequences of KS domain facilitated to distinguish *B. atrophaeus* SHB2097 from the *B. velezensis* SHB2098 strains that could not be realized by 16S rRNA-built phylogenetic method.

For analyzing the presence of antimicrobial compounds, spectroscopic features of the solvent extract of *B. atrophaeus* SHB2097 were evaluated by proton nuclear resonance spectroscopic (^{1}H NMR) study. ^{1}H NMR spectrum were apportioned to different characteristic sections, wherein a greater proton integral (> 150) at δ 0.5–2.0 in the organic extract was recorded. The number of protons (~ 50) at δ 2.1–2.5 were apportioned to acetyl or allylic groups, whereas weaker proton integrals (~ 23) at δ 2.6–3.5 displayed the appearance of alkoxyl functionality. Marked proton integrals at olefinic region (δ 4.6–6.0, 58.49) also depicted the presence of unsaturation in the compounds present in the organic extract (Fig. S6). Detailed purification and structure characterization of the organic extract will form a part of separate study.

Hemolysis activity of the isolate *B. atrophaeus* SHB2097 was analyzed with different set of hemolysis primers, wherein negative result recognized the isolate as non-pathogenic. Sporulation assessment indicated that the isolate *B. atrophaeus* SHB2097 has spore-forming capacity (1.29×10^8 cfu/mL).

Siderophores are bacterial iron-chelating metabolites synthesized by *nrps* or *pks* domains, to scavenge iron from surroundings (Kramer et al. 2020), thereby augmenting their antagonistic properties against competing pathogens. The current study revealed that the heterotrophic *B. atrophaeus* SHB2097 could produce siderophore on the CAS agar plates (Fig. 4) with a hallow of about 32 mm. Presence of siderophore biosynthetic gene in the genome assembly of *B. atrophaeus* SHB2097 further corroborated the CAS assay results (Fig. 4). Reactive oxygen species (ROS) are intermediates in metabolic reactions embodying the mitochondrial electron transport, in which reduced form of Fe^{2+} ion could promulgate the radical chain reaction by losing/acquiring the electrons. As a result, the attenuation to develop ROS could be carried out by Fe^{2+} chelation property of the organic extract of *B. atrophaeus* SHB2097 (IC_{50} 4.2 µg/mL), thus contributing to its antioxidant property. Therefore, assembly of siderophores and their biosynthetic genes (accession numbers of MZ222387 and MZ222388) in tandem with Fe^{2+} chelation ability acknowledged its potential to scavenge Fe^{2+} ion from ambiences, and as a result could effectively antagonize the pathogens in consort with attenuating the buildup of ROS. Moreover, siderophore antibiotics could be transported into the Gram-negative bacterial cells at ease by using Fe^{2+} accretion pathways (Gram et al. 1999).

The bacterial growth curve of *B. atrophaeus* SHB2097 was found to be proportional to the inhibition curve, which recognized that the presence of greater number of cells could result in the production of more secondary metabolites. The crude organic (ethyl acetate) extract of *B. atrophaeus* SHB2097 displayed antagonism against a wide spectra of nosocomial pathogens, for example MRSA (skin infection), *E. coli* (gastrointestinal), *S. pyogenes* (skin), *E. tarda* (myonecrosis and gastrointestinal), *V. parahemolyticus* (gastrointestinal), and VREfs (sepsis and meningitis). Organic extract of *B. atrophaeus* SHB2097 revealed noteworthy antibacterial potential against the pathogens (zone of inhibition 28–38 mm), compared to that exhibited by chloramphenicol (8–15 mm) (Fig. 4B–D). Notably, MIC and MBC of the organic extracts were comparable or better than those displayed by chloramphenicol. The MIC of the organic extract was 6.25 µg/mL against *V. parahemolyticus,* MRSA, *A. salmonicida* (ATCC 27,013), *Y. enterocolitica* (MTCC 859), and *A. hydrophila* (ATCC 7966) (Table 4), wherein chloramphenicol displayed a comparable MIC (6.25 µg/mL). The crude extract fared better than the standard antibiotics (MIC 12.5 µg/mL) against vancomycin-resistant *S. aureus,* *E. coli* (MTCC 443), and *A. hydrophila* (ATCC 7966) showing the MIC of 6.25 µg/mL.

Conclusion

Need for newer sources of antibiotics due to the increasing antibiotic resistance has resulted into the expanded use of bioactives from novel natural origins. Seaweeds are prospective host organisms for the associated heterotrophic bacteria. In this study, heterotrophic *B. atrophaeus* SHB2097 was isolated from the marine macroalga exhibited potential iron-chelating and antimicrobial activities, which were reinforced by the presence of *pks*, *nrps* and siderophore biosynthetic genes, and therefore, could be studied for cutting-edge pharmacological applications. It could be inferred that antimicrobial properties could not be exclusively judged by metagenomic analyses, considering that a number of strains might get away with the amplification of the anticipated genes. It follows that the antibacterial properties could solely be weighed by evaluating the attenuation potential of the anticipated indicator organism. We also vouch for metabolite gene-centered screening of heterotrophs for using biosynthetic gene clusters. Future studies regarding isolation and characterization of antimicrobial compounds from *B. atrophaeus* SHB2097 would be attempted for development of potential antibiotic agents.

GenBank accession numbers

Partial 16S rRNA gene sequences of *B. atrophaeus* and *B. velezensis* were submitted in NCBI GenBank (accession of MW821482, MW821799). Partial *pks* sequences corresponding to *B. atrophaeus* MW821482 were deposited under the accession of MZ222383, MZ222384, MZ222385, MZ222386, whereas *nrps* gene sequence was deposited in the Genbank as MZ222389. Coding sequences for siderophore biosynthetic genes were deposited under the accession numbers MZ222387 and MZ222388.

Supplementary Information The online version contains supplementary material available at https://doi.org/10.1007/s00203-022-02784-2.

Acknowledgements This work was funded by the Indian Council of Agricultural Research (ICAR) under the project titled as "Development of Bioactive Pharmacophores from Marine Organisms" (grant number MBT/HLT/SUB23). The authors thank the Director, Central Marine Fisheries Research Institute and Head, Marine Biotechnology Division, Central Marine Fisheries Research Institute for facilitating the research activities. The authors thank the Dean, School of Biotechnology, Amrita Vishwa Vidyapeetham for supporting CV.

Author contributions KC and CV conceived and designed research, acquired funds, and conducted experiments. KC, RDC, and SA analyzed data. All authors drafted and approved the manuscript.

Funding This study was funded by the Indian Council of Agricultural Research (ICAR).

Declarations

Conflict of interest No potential conflict of interest was reported by the authors. This article does not contain any studies with human participants or animals performed by any of the authors.

References

Aleti G, Sessitsch A, Brader G (2015) Genome mining: prediction of lipopeptides and polyketides from *Bacillus* and related Firmicutes. Comput Struct Biotechnol J 13:192–203. https://doi.org/10.1016/j.csbj.2015.03.003

Ali AIB, Bour ME, Ktari L, Bolhuis H, Ahmed M, Boudabbous A, Stal LJ (2012) *Jania rubens*-associated bacteria molecular identification and antimicrobial activity. J Appl Phycol 24(3):525–534

Armstrong E, Yan L, Boyd KG, Wright CP, Burgess JG (2001) The symbiotic role of marine microbes on living surfaces. Hydrobiologia 461:37–40

Bauer AW, Kirby WM, Sherris JC, Turck M (1966) Antibiotic susceptibility testing by a standardized single disk method. Am J Clin Pathol 45(4):493–496

Brakhage AA (2012) Regulation of fungal secondary metabolism. Nat Rev Microbiol 11(1):21–32

Chakraborty K, Thilakan B, Raola VK (2014) Polyketide family of novel antibacterial 7-*O*-methyl-5'-hydroxy-3'-heptenoate-macrolactin from seaweed-associated *Bacillus subtilis* MTCC 10403. J Agric Food Chem 62(50):12194–12208

Chakraborty K, Thilakan B, Kizhakkekalm VK (2017) Antibacterial aryl-crowned polyketide from *Bacillus subtilis* associated with seaweed *Anthophycus longifolius*. J Appl Microbiol 124(1):108–125

Chakraborty K, Francis A, Chakraborty RD, Asharaf S, Kizhakkekalam VK, Paulose SK (2021) Marine macroalga-associated heterotrophic *Bacillus velezensis*: a novel antimicrobial agent with siderophore mode of action against drug-resistant nosocomial pathogens. Arch Microbiol 203(9):5561–5575

Chassagne F, Cabanac G, Hubert G, David B, Marti G (2019) The landscape of natural product diversity and their pharmacological relevance from a focus on the Dictionary of Natural Products®. Phytochem Rev 18(3):601–622

Chen L, Heng J, Qin S, Bian K (2018) A comprehensive understanding of the biocontrol potential of *Bacillus velezensis* LM2303 against *Fusarium* head blight. PLoS ONE 13(6):e0198560

Cherian T, Yalla S, Mohanraju R (2019) Antimicrobial potential of methanolic extract of *Bacillus aquimaris* isolated from the marine waters of Burmanallah coast, South Andaman. Int J Biopharm Res 8(12):2806–2813

Datta B, Chakrabartty PK (2014) Siderophore biosynthesis genes of *Rhizobium* sp. isolated from *Cicer arietinum* L. 3 Biotech 4(4):391–401

Doekel S, Coëffet-Le Gal MF, Gu JQ, Chu M, Baltz RH, Brian P (2008) Non-ribosomal peptide synthetase module fusions to produce derivatives of daptomycin in *Streptomyces roseosporus*. Microbiology 154:2872–2880. https://doi.org/10.1099/mic.0.2008/020685-0

Felnagle EA, Jackson EE, Chan YA, Podevels AM, Berti AD, McMahon MD, Thomas MG (2008) Nonribosomal peptide synthetases involved in the production of medically relevant natural products. Mol Pharm 5:191–211. https://doi.org/10.1021/mp700137g

Fickers P (2012) Antibiotic compounds from *Bacillus*: why are they so amazing? Am J Biochem Biotechnol 8(1):40–46

Francis A, Chakraborty K (2021) Marine macroalgae-associated heterotroph *Bacillus velezensis* as prospective therapeutic agent. Arch Microbiol 203(4):1671–1682

Gao Q, Tomlinson G, Das S, Cummings S, Sveen L, Fackenthal J, Schumm P, Olopade OI (2000) Prevalence of BRCA1 and BRCA2 mutations among clinic-based African American families with breast cancer. Hum Genet 107(2):186–191

Goecke F, Labes A, Wiese J, Imhoff JF (2010) Chemical interactions between marine macroalgae and bacteria. Mar Ecol Prog Ser 409:267–299

Gram L, Melchiorsen J, Spanggaard B, Huber I, Nielsen TF (1999) Inhibition of *Vibrio anguillarum* by *Pseudomonas fluorescens* AH2, a possible probiotic treatment of fish. Appl Environ Microbiol 65(3):969–973

Gram L, Melchiorsen J, Bruhn JB (2010) Antibacterial activity of marine culturable bacteria collected from a global sampling of ocean surface waters and surface swabs of marine organisms. Mar Biotechnol 12(4):439–451

Gülçin I (2007) Comparison of in vitro antioxidant and antiradical activities of L-tyrosine and L-dopa. Amino Acids 32(3):431–438

Hwang JY, Park JH (2015) Characteristics of enterotoxin distribution, hemolysis, lecithinase, and starch hydrolysis of *Bacillus cereus* isolated from infant formulas and ready-to-eat foods. J Dairy Sci 98:1652–1660. https://doi.org/10.3168/jds.2014-9042

Ismail AF, Ktari L, Ahmed M, Bolhuis H, Bouhaouala-Zahar B, Stal LJ, Boudabbous A, Bour ME (2018) Heterotrophic bacteria associated with the green alga *Ulva rigida*: identification and antimicrobial potential. J Appl Phycol 30(5):2883–2899

Jones DT, Taylor WR, Thornton JM (1992) The rapid generation of mutation data matrices from protein sequences. Comput Appl Biosci 8(3):275–282

Kanagasabhapathy M, Sasaki H, Haldar S, Yamasaki S, Nagata S (2006) Antibacterial activities of marine epibiotic bacteria isolated from brown algae of Japan. Ann Microbiol 56(2):167–173

Kanagasabhapathy M, Sasaki H, Nagata S (2008) Phylogenetic identification of epibiotic bacteria possessing antimicrobial activities isolated from red algal species of Japan. World J Microbiol Biotechnol 24(10):2315–2321

Kim SY, Lee SY, Weon HY, Sang MK, Song J (2017) Complete genome sequence of *Bacillus velezensis* M75, a biocontrol agent against fungal plant pathogens, isolated from cotton waste. J Biotechnol 241:112–115

Kizhakkekalam VK, Chakraborty K (2019) Pharmacological properties of marine macroalgae-associated heterotrophic bacteria. Arch Microbiol 201(4):505–518

Kizhakkekalam VK, Chakraborty K (2020) Marine macroalgae-associated heterotrophic *Firmicutes* and *Gammaproteobacteria*: prospective anti-infective agents against multidrug resistant pathogens. Arch Microbiol 202(4):905–920

Kizhakkekalam VK, Chakraborty K, Joy M (2020) Oxygenated elansolid-type of polyketide spanned macrolides from a marine heterotrophic *Bacillus* as prospective antimicrobial agents against multidrug-resistant pathogens. Int J Antimicrob Agents 55(3):105892

Kramer J, Özkaya Ö, Kümmerli R (2020) Bacterial siderophores in community and host interactions. Nat Rev Microbiol 18(3):152–163

Krieg NR, Holt JG (1984) Bergey's manual of systematic bacteriology, 1st edn. Williams and Wilkins Co, Baltimore, pp 161–172

Kubanek J, Jensen PR, Keifer PA, Sullards MC, Collins DO, Fenical W (2003) Seaweed resistance to microbial attack: a targeted chemical defense against marine fungi. Proc Natl Acad Sci USA 100(12):6916–6921

Kumar S, Stecher G, Li M, Knyaz C, Tamura K (2018) MEGA X: molecular evolutionary genetics analysis across computing platforms. Mol Biol Evol 35(6):1547–1549

Le Lann K, Surget G, Couteau C, Coifard L, Cerantola S, Gaillard F, Larnicol M, Zubia M et al (2016) Sunscreen, antioxidant, and bactericide capacities of phlorotannins from the brown macroalga *Halidrys siliquosa*. J Appl Phycol 28(6):3547–3559

Lemos ML, Toranzo AE, Barja JL (1985) Antibiotic activity of epiphytic bacteria isolated from intertidal seaweeds. Microb Ecol 11(2):149–163

Li X, Gao X, Zhang S, Jiang Z, Yang H, Liu X, Jiang Q, Zhang X (2020) Characterization of a *Bacillus velezensis* with antibacterial activity and inhibitory effect on common aquatic pathogens. Aquaculture 523:735165

Longford S, Tujula N, Crocetti GR, Holmes AJ, Holmstrom C, Kjelleberg S, Steinberg P, Taylor MW (2007) Comparisons of diversity of bacterial communities associated with three marine eukaryotes. Aquat Microb Ecol 48(3):217–229

Louden BC, Haarmann D, Lynne AM (2011) Use of blue agar CAS assay for siderophore detection. J Microbiol Biol Educ 12:51–53. https://doi.org/10.1128/jmbe.v12i1.249

Nicholson WL, Setlow P (1990) Dramatic increase in negative superhelicity of plasmid DNA in the forespore compartment of sporulating cells of *Bacillus subtilis*. J Bacteriol 172(1):7–14

Pandey A (2019) Pharmacological potential of marine microbes. In: Arora D, Sharma C, Jaglan S, Lichtfouse E (eds) Pharmaceuticals from microbes. Environmental chemistry for a sustainable world, 28th edn. Springer, Cham, pp 1–25

Penesyan A, Marshall-Jones Z, Holmstrom C, Kjelleberg S, Egan S (2009) Antimicrobial activity observed among cultured marine epiphytic bacteria reflects their potential as a source of new drugs. FEMS Microbiol Ecol 69(1):113–124

Sastalla I, Fattah R, Coppage N, Nandy P, Crown D, Pomerantsev AP, Leppla SH (2013) The *Bacillus cereus* hbl and nhe tripartite enterotoxin components assemble sequentially on the surface of target cells and are not interchangeable. PLoS One 8:e76955. https://doi.org/10.1371/journal.pone.0076955

Schirmer A, Gadkari R, Reeves CD, Ibrahim F, DeLong EF, Hutchinson CR (2005) Metagenomic analysis reveals diverse polyketide synthase gene clusters in microorganisms associated with the marine sponge *Discodermia dissoluta*. Appl Environ Microbiol 71(8):4840–4849

Seng P, Drancourt M, Gouriet F, La-Scola B, Fournier PE, Rolain JM, Raoult D (2009) Ongoing revolution in bacteriology: routine identification of bacteria by matrix-assisted laser desorption ionization time-of-fight mass spectrometry. Clin Infect Dis 49(4):543–551

Singh RP, Mantri VA, Reddy CRK, Jha B (2011) Isolation of seaweed-associated bacteria and their morphogenesis-inducing capability in axenic cultures of the green alga *Ulva fasciata*. Aquat Biol 12(1):13–21

Soria-Mercado IE, Villarreal-Gómez LJ, Rivas GG, Sánchez NEA (2012) Bioactive compounds from bacteria associated to marine algae. Biotechnology molecular studies and novel application for improved quality of human life. InTech, Croatia, pp 25–44

Tamura K, Peterson D, Peterson N, Stecher G, Nei M, Kumar S (2011) MEGA5: molecular evolutionary genetics analysis using maximum likelihood, evolutionary distance, and maximum parsimony methods. Mol Biol Evol 28(10):2731–2739

Thilakan B, Chakraborty K, Chakraborty RD (2016) Antimicrobial properties of cultivable bacteria associated with seaweeds in the Gulf of Mannar on the southeast coast of India. Can J Microbiol 62(8):668–681

Turick CE, Caccavo F Jr, Tisa LS (2008) Pyomelanin is produced by *Shewanella algae* BrY and affected by exogenous iron. Can J Microbiol 54(4):334–339

Vijayalakshmi S, Ramasamy MS, Murugesh S, Murugan A (2008) Isolation and screening of marine associated bacteria from Tamil Nadu, Southeast coast of India for potential antibacterial activity. Ann Microbiol 58(4):605–609

Wang H, Fewer DP, Holm L, Rouhiainen L, Sivonen K (2014) Atlas of nonribosomal peptide and polyketide biosynthetic pathways reveals common occurrence of nonmodular enzymes. Proc Natl Acad Sci USA 111(25):9259–9264

Whelan S, Goldman N (2001) A general empirical model of protein evolution derived from multiple protein families using a maximum-likelihood approach. Mol Biol Evol 18(5):691–699

Wiese J, Thiel V, Nagel K, Staufenberger T, Imhof JF (2009) Diversity of antibiotic-active bacteria associated with the brown alga *Laminaria saccharina* from the Baltic Sea. Mar Biotechnol 11(2):287–300

Winter JM, Chiou G, Bothwell IR, Xu W, Garg NK, Luo M, Tang Y (2013) Expanding the structural diversity of polyketides by exploring the cofactor tolerance of an inline methyltransferase domain. Org Lett 15(14):3774–3777

Xia J, Sinelnikov IV, Han B, Wishart DS (2015) MetaboAnalyst 3.0-making metabolomics more meaningful. Nucleic Acids Res 43(W1):W251–W257

Yi Y, Zhang Z, Zhao F, Liu H, Yu L, Zha J, Wang G (2018) Probiotic potential of *Bacillus velezensis* JW: antimicrobial activity against fish pathogenic bacteria and immune enhancement effects on *Carassius auratus*. Fish Shellfish Immunol 78:322–330

Zhang W, Zhang F, Li Z, Miao X, Meng Q, Zhang X (2009) Investigation of bacteria with polyketide synthase genes and antimicrobial activity isolated from South China Sea sponges. J Appl Microbiol 107(2):567–575

Zhao K, Penttinen P, Guan T, Xiao J, Chen Q, Xu J, Lindström K, Zhang L, Zhang X, Strobel GA (2011) The diversity and antimicrobial activity of endophytic actinomycetes isolated from medicinal plants in Panxi plateau, China. Curr Microbiol 62(1):182–190. https://doi.org/10.1007/s00284-010-9685-3

Zheng L, Han X, Chen H, Lin W, Yan X (2005) Marine bacteria associated with marine macro organisms: the potential antimicrobial resources. Anal Microbial 55(2):119–124

Zhu P, Zheng Y, You Y, Yan X, Shao J (2009) Molecular phylogeny and modular structure of hybrid NRPS/PKS gene fragment of *Pseudoalteromonas* sp. NJ6–3–2 isolated from marine sponge *Hymeniacidon perleve*. J Microbiol Biotechnol 19(3):229–237

Zubia M, Fabre MS, Kerjean V, Lann KL, Pouvreau VS, Fauchon M, Deslandes E (2009) Antioxidant and antitumoural activities of some Phaeophyta from Brittany coasts. Food Chem 116(3):693–701